

Assessment of the Peroxisomal Redox State in Living Cells Using NADPH- and NAD⁺/NADH-Specific Fluorescent Protein Sensors

Cláudio F. Costa¹, Hongli Li¹, Mohamed A. F. Hussein^{1,2}, Yi Yang^{3,4}, Celien Lismont¹, and Marc Fransen^{1,*}

¹Laboratory of Peroxisome Biology and Intracellular Communication, Department of Cellular and Molecular Medicine, KU Leuven, Belgium

²Department of Biochemistry, Faculty of Pharmacy, Assiut University, Asyut, Egypt

³Synthetic Biology and Biotechnology Laboratory, State Key Laboratory of Bioreactor Engineering, Shanghai Collaborative Innovation Center for Biomanufacturing Technology, East China University of Science and Technology, Shanghai, China.

⁴State Key Laboratory of Neuroscience, CAS Center for Excellence in Brain Science, Institute of Neuroscience, Chinese Academy of Sciences, Shanghai, China.

*Correspondence

marc.fransen@kuleuven.be

Running head

Dynamic Monitoring of Pyridine Nucleotides in Peroxisomes

Abstract

The pyridine nucleotides NAD(H) and NADP(H) are key molecules in cellular metabolism and measuring their levels and oxidation states with spatiotemporal precision is of great value in biomedical research. Traditional methods to assess the redox state of these metabolites are intrusive and prohibit live-cell quantifications. This obstacle was surpassed by the development of genetically encoded fluorescent biosensors enabling dynamic measurements with subcellular

resolution in living cells. Here, we provide step-by-step protocols to monitor the intraperoxisomal NADPH levels and NAD⁺/NADH redox state in cellulo by using targeted variants of iNAP1 and SoNar, respectively.

Key Words

Peroxisomes, NAD(H), NADP(H), Redox state, Live-cell imaging, Fluorescent biosensors, SoNar, iNAP

1 Introduction

Nicotinamide adenine dinucleotides are abundant soluble cofactors that play a pivotal role in a wide range of biological processes including, among others, energy production, redox homeostasis, ion channel regulation, and cell signaling (*1, 2*). For example, many dehydrogenases involved in biochemical pathways such as glycolysis and the Krebs cycle use NAD⁺ as electron acceptor to catalyze the oxidation of their substrate(s), thereby generating NADH (*3*). In mitochondria, NADH donates a pair of electrons to complex I of the respiratory chain for ATP synthesis and is hence regenerated to NAD⁺ (*4*). NAD⁺ can also serve as a cofactor for enzymes such as mono-ADP-ribose transferases, poly(ADP-ribose) polymerases, and sirtuins, thereby indirectly regulating the transcription of epigenetically modified genes (*1, 5*). In some processes, NADPH is playing a crucial role as redox cofactor. For example, this molecule is required to drive the activities of glutathione reductase, thioredoxin reductases, and NADPH oxidases (*1*). NADPH is primarily regenerated from NADP⁺ via the oxidative branch of the pentose phosphate pathway (*4*). Perturbations in the metabolism of pyridine nucleotides have been associated with oxidative stress-related parameters (e.g., DNA damage, mitochondrial dysfunction, and inflammation) and disease (e.g., accelerated aging and cancer) (*4, 6, 7*).

Given the relevance of pyridine nucleotides in cell physiology and human health, methods to measure these redox carriers are of great value for biomedical research. Traditional biochemical

methods include colorimetric enzymatic assays (8, 9), capillary electrophoresis (10), high-pressure liquid chromatography with UV or fluorescence detection (11, 12, 13), nuclear magnetic resonance (14), and liquid chromatography with tandem mass spectrometry (15, 16, 17).

However, these methods typically involve cell lysis, making them unsuitable for real-time in vivo measurements. In addition, as fractionation techniques can result in metabolite leakage (18), such intrusive methodologies are inadequate for metabolite measurements at the subcellular level.

Furthermore, given that pyridine nucleotides display distinct chemical stability in different biological matrices and are particularly sensitive to auto-oxidation, accurately quantifying them represents an analytical challenge (17). To cope with these shortcomings, multiple genetically encoded fluorescent sensors have been developed that allow rapid, sensitive, and specific bioimaging of pyridine nucleotide dynamics in living cells at a subcellular level (19).

SoNar is a fusion of circularly permuted yellow fluorescent protein (cpYFP) and the NADH-binding domain of the redox-sensing transcriptional repressor Rex from *Thermus aquaticus* (T-Rex) that, upon binding to NAD⁺ or NADH, exhibits two different conformational states, thereby affecting its spectral properties (20, 21). While the sensor emission peak is always located near 518 nm, the excitation peak shifts from 485 nm to 420 nm upon the exchange of NAD⁺ with NADH (Fig. 1). As such, SoNar functions as an intrinsically ratiometric sensor that can be used to infer the local oxidation state of the NAD⁺/NADH redox couple by measuring the fluorescence intensity of the sensor after excitation around 420 and 485 nm. Importantly, the sensor is strictly responsive to the free NAD⁺/NADH ratio and not to the concentration of these molecules.

The iNAP1 sensor is a mutated form of SoNar in which the NADH binding domain of T-Rex was engineered to convert the sensor into an NADPH binder (22). Like SoNar, iNAP1 presents different conformational states and fluorescence excitation spectra depending on whether it is bound or not to NADPH. Specifically, upon NADPH binding, the sensor shows an excitation peak around 420 nm that is absent in the NADPH-free form (Fig. 1). Therefore, it is possible to

infer changes in the free NADPH levels by measuring the fluorescence intensities of iNAP1 likewise what is done for SoNar (22).

Importantly, given that (i) both iNAP1 and SoNar are cpYFP-based sensors, and (ii) cpYFP is highly pH sensitive (23), it is necessary to control and compensate for any potential pH changes by measuring in parallel the responses of pyridine nucleotide-insensitive but pH-sensitive fluorescent proteins such as cpYFP and iNAPc. These proteins display similar pH sensitivity as SoNar and iNAP1, respectively (20, 22).

In this chapter, we detail the use of SoNar and iNAP to track, respectively, subtle changes in the free NAD⁺/NADH ratios and NADPH levels inside peroxisomes. The protocols can be easily adapted depending on the purpose of the study (e.g., to study the time-dependent changes of these metabolites upon a specific cell treatment). This makes SoNar and iNAP1 valuable tools for the peroxisome biology research field.

2 Materials

2.1 Cell Culture

2.1.1 Equipment

1. Biosafety cabinet.
2. Humidified CO₂ incubator (95% air, 5% CO₂, 37°C).
3. Vacuum aspiration system.
4. Inverted light microscope (200-fold magnification).
5. Mammalian cell counter.
6. 37°C water bath.
7. Tabletop centrifuge equipped with a swing-out rotor for 15-ml conical tubes.
8. Sterile Pasteur pipettes.

9. Disposable sterile serological pipettes.
10. Micropipettes.
11. Sterile micropipette filter tips.

2.1.2 Materials

1. Cells: Flp-In™ T-REx™ 293 (ThermoFisher Scientific, R78007) (*see Note 1*).
2. Complete growth medium: alpha-modified minimum essential medium (MEM α) supplemented with 10% (v/v) fetal bovine serum (FBS), 2 mM UltraGlutamine, and 1 \times MycoZap Plus-CL (*see Note 2*). Store at 4°C.
3. T-25 cell culture flasks.
4. Dulbecco's phosphate-buffered saline (DPBS) without Ca²⁺ and Mg²⁺ (DPBS^{-Ca,-Mg}). Store at 4°C.
5. Trypsin-EDTA (1x): 0.05% (w/v) trypsin, 0.02% (w/v) EDTA (in DPBS^{-Ca,-Mg}) (*see Note 3*). Store at -20°C (*see Note 4*).
6. 70% (v/v) ethanol.
7. Mycoplasma-Off™ (Minerva Biolabs, 15-5000).

2.2 Electroporation

1. Neon Transfection System, including the electroporation device, pipette station, pipette, 10 μ l tips, electroporation tubes, electrolytic buffer E, and resuspension buffer R (Thermo Fisher Scientific) (*see Note 5*).
2. Cell transfection medium: complete growth medium without MycoZap Plus-CL. Store at 4°C.
3. Plasmids (1 μ g/ μ L in deionized water; *see Note 6*) encoding LbNOX (Addgene #75285) or peroxisome-targeted (po-) variants of SoNar, cpYFP, iNAP, iNAPc, or mCherry (*see Notes 7 and 8*).

4. Glass-bottomed FluoroDish cell culture dishes – 35 mm (World Precision Instruments, FD35).
5. Polyethyleneimine (PEI) (molecular mass range of 50–100 kDa).
6. Filter-sterilized 150 mM NaCl.
7. PEI-coated FD35 Fluorodishes (*see Note 9*).
8. 200 mM dehydroepiandrosterone (DHEA) in cell culture grade DMSO.
9. Sterile microtubes.

2.3 Fluorescence Microscopy

1. Live-cell imaging station (Olympus): inverted IX-81 microscope, controlled by cellSens Dimension software and equipped with (i) a motorized stage, (ii) a temperature-, humidity-, and CO₂-controlled incubation chamber, (iii) a pE-4000 illumination system, (iv) a UPlanSApo 100x/1.40 oil immersion objective, (v) an F420 filter cube (excitation: 405/20 nm; dichroic mirror: 505 nm; emission: 530/20 nm), (vi) an F485 filter cube (excitation: 482.5/25 nm; dichroic mirror: 505 nm; emission: 530/20 nm), (vii) a Texas Red filter cube (excitation: 562.5/35 nm; dichroic mirror: 600 nm; emission: 610 nm long pass), (viii) a DP73 high-performance Peltier-cooled digital color camera, and (ix) an insert for 35 mm dishes (*see Note 10*).
2. 5% CO₂/air mixture.
3. Immersion oil Type-F.

3 Methods

Similar cell culture and electroporation protocols have already been published in former issues of this journal (24, 25). However, to provide the reader with all the practical information needed to successfully carry out the NADPH and NAD⁺/NADH measurements, these procedures are described again.

3.1 Cell Culture

1. Turn the biosafety cabinet on for at least 5 minutes prior to starting work.
2. Decontaminate the work surface of the biosafety cabinet with 70% (v/v) ethanol and Mycoplasma-Off™ solution.
3. Clean all materials with 70% ethanol before entering the biosafety cabinet (*see Note 11*).
4. Culture the Flp-In™ T-REx™ 293 cells in a complete growth medium (5 mL/T-25 cell culture flask) in a humidified CO₂ incubator (95% air, 5% CO₂, 37°C).
5. Refresh the cell culture medium every 2 to 3 days.
6. Split the cells before they reach 100% confluency (*see steps 7 to 13 and Note 12*).
7. Prewarm DPBS^{-Ca,-Mg}, trypsin-EDTA, and complete growth medium to 37°C.
8. Aspirate the medium from the cell culture flask with a Pasteur pipette by vacuum aspiration and wash the cells once with 5 mL of DPBS^{-Ca,-Mg}.
9. Add enough trypsin-EDTA solution to the cells to cover the bottom surface (1 mL/T-25 flask).
10. Aspirate the Trypsin-EDTA solution and incubate the cells at room temperature or 37°C for 2 to 5 minutes or until cell detachment is observed (*see Note 13*).
11. Upon detachment, resuspend the cells in a complete growth medium (5 mL/T-25 flask) (*see Note 14*).
12. Pipette the cell suspension three times up and down to disperse all cell clumps.
13. Transfer the desired amount of cell suspension to a new T-25 cell culture flask and add fresh medium to a final volume of 5 mL.

3.2 Neon electroporation of Flp-In™ T-REx™ 293 cells

3.2.1 Preparation of the Cells

1. Culture the required number of cells ($\sim 5 \times 10^4$ cells/electroporation) in a complete growth medium (*see Section 3.1*).

2. Trypsinize the cells (*see Section 3.1, steps 7 to 12*, but use prewarmed complete growth medium as harvest medium) (*see Note 15*).
3. Transfer the cell suspension to a 15-ml conical tube and take an aliquot of the suspension for cell counting.
4. Centrifuge the cell suspension at 300 x g for 5 min (at room temperature).
5. Remove the supernatant and resuspend the cell pellet in 10 mL of D-PBS^{-Ca,-Mg}.
6. Pellet the cells again (*see step 4*).
7. Carefully aspirate the supernatant and resuspend the cells in resuspension buffer R at a final density of 5×10^6 cells/ml (*see Notes 16-17*).
8. Gently pipette the cell suspension 5x up and down to avoid cell clumps that may reduce transfection efficiency.

3.2.2 Electroporation of the Cells

1. Place the Neon pipette station in the biosafety cabinet.
2. Set the pulse parameters (1150 V, 20 ms pulse width, 2 pulses) on the electroporation device (*see Note 18*).
3. For each condition, add 1.5 mL of prewarmed transfection medium into an FD35 Fluorodish (*see Note 19*).
4. Fill a Neon tube with 3 mL of electrolytic buffer E and place it into the pipette station.
5. Gently transfer 20 μ l of the cell suspension and 2 μ l of plasmid DNA (1 μ g/ μ l) to a sterile microtube and mix by pipetting once up and down.
6. Mount a 10 μ l Neon tip onto the Neon pipette.
7. Slowly aspirate 10 μ l of the cell-DNA mixture. Make sure there are no air bubbles in the tip.
8. Insert the pipette into the Neon tube in the pipette station and press start on the touch screen of the electroporation device.

9. After the electrical pulses have been applied, remove the pipette from the pipette station and immediately transfer the tip content to the FD35 Fluorodish.
10. Repeat steps 7 to 9.
11. Place the Neon tip in an appropriate biological hazardous waste container (*see Note 5*).
12. Subject the FD35 Fluorodish to a gentle cross-like movement to achieve an even cell distribution.
13. Repeat steps 5 to 12 for the remaining cell-DNA mixtures.
14. Put the FD35 Fluorodishes in a humidified CO₂ incubator (95% air, 5% CO₂, 37°C) to allow the cells to attach to the PEI-coated glass bottom surface (*see Note 20*).
15. Upon cell attachment, change the medium to complete growth medium containing antibiotics.
16. Culture the cells in the humidified CO₂ incubator until analysis (*see Note 21*).

3.3 Pyridine Nucleotide Measurements and Analysis

3.3.1 Preparing for Live-Cell Imaging

1. Prewarm the assay medium to 37°C (*see Note 22*).
2. Aspirate the culture medium from the FD35 Fluorodish, rinse the cells once with prewarmed assay medium, and add 1.5 mL of the same medium.
3. Incubate the cells for at least 1 h in a humidified CO₂ incubator (95% air, 5% CO₂, 37°C).
4. Switch on the temperature-, humidity-, and CO₂-controlled incubation chamber of the live-cell imaging station at least 1 h before image acquisition (*see Note 23*).
5. Switch on all other components of the live-cell imaging system.

3.3.2 Image Collection

1. Place a small drop of immersion oil on the 100x objective and place the FD35 FluoroDish in the dish holder.

2. Select the appropriate microscope settings to detect the fluorescent biosensor and collect images of the cells (*see* Table 1 and **Notes 24-27**).
3. Repeat steps 1 and 2 for the remaining conditions.

3.3.3 Image Analysis

1. Subtract the background in both channels by using the signal intensity of a cell-free area as a reference value (*see* **Note 28**).
2. Select a minimum of 20 regions of interest (ROIs), preferably in different cells (*see* **Notes 29-31**).
3. Measure the signal intensities of the ROIs in both channels.
4. Calculate the fluorescence ratios by dividing the F485 values by the F420 values.
5. Correct for potential pH effects by dividing the individual F485/F420 ratios obtained for SoNar and iNAP1 by the mean F485/F420 ratio of cpYFP and iNAPc, respectively.
6. Analyze the data statistically (*see* **Notes 32-34**).
7. Visualize the results in your preferred manner (e.g., box plots).

3.4 Functional validation of po-SoNar

1. Culture Flp-InTM T-RExTM 293 cells (*see* **Section 3.1**).
2. Electroporate the cells with plasmids encoding po-SoNar or po-cpYFP, both in the absence or presence of a plasmid encoding LbNOX (*see* **Section 3.2** and **Note 35**).
3. Collect and analyze images of the fluorescent biosensors (*see* **Section 3.3** and **Fig. 3A**).

3.5 Functional validation of po-iNAP1

1. Culture Flp-InTM T-RExTM 293 cells (*see* **Section 3.1**).
2. Electroporate the cells with plasmids encoding po-iNAP1 or po-iNAPc (*see* **Section 3.2**).
3. Collect images of the fluorescent biosensors (*see* **Sections 3.3.1** and **3.3.2**).

4. Aspirate the culture medium from the FD35 Fluorodishes, rinse the cells once with prewarmed assay medium, and add 1.5 mL of the same medium containing 200 μ M DHEA (*see Note 36*).
5. Incubate the cells for 30 min in the humidified CO₂ incubator.
6. Collect images of the fluorescent biosensors (*see Sections 3.3.1 and 3.3.2*).
7. Analyze the images (*see Section 3.3.3 and Fig. 3B*).

4 Notes

1. The protocols in this chapter are optimized for Flp-In™ T-REx™ 293 cells. However, depending on the purpose of the study, any other transfectable cell line can be used as long as appropriate cell culture and transfection protocols are implemented.
2. Cells can be grown in different media. However, given that cellular metabolism and redox state are intricately linked (26), different cell culture media may affect the outcome of the measurements.
3. The optimal concentration and incubation time of trypsin can vary according to cell type and density.
4. Repeated freezing and thawing will reduce the enzymatic activity and should be avoided.
5. To reduce the costs, the electroporation tips and tubes can be recycled, and the electrolyte and resuspension buffers can be replaced by a homemade RF1 buffer (250 mM sucrose, 1 mM MgCl₂; in DPBS) (27).
6. Use your own preferred procedure to isolate transfection-quality plasmid DNA.
7. As for po-mCherry (28), the mammalian expression plasmids encoding po-SoNar, po-iNAP1, or po-iNAP were designed to append KSKL, the prototypic C-terminal targeting signal for peroxisomal matrix proteins, to their C-terminus. Given that this strategy was not successful for cpYFP, a plasmid encoding a fusion protein comprising the (cleavable) N-terminal targeting signal of rat peroxisomal 3-ketoacyl-CoA thiolase and cpYFP was constructed.
8. Researchers who want to obtain these plasmids must first sign a material transfer agreement with (i) Dr. Yi Yang (East China University of Science and Technology,

- Shanghai, China; e-mail: yiyang@ecust.edu.cn) to formally accept all conditions and restrictions for each DNA template, and (ii) Dr. Marc Fransen (KU Leuven, Leuven, Belgium; e-mail: marc.fransen@kuleuven.be) to obtain the plasmids described in this chapter.
9. Cover the surface of an FD35 Fluorodish with 1 mL of filtered-sterilized PEI (25 µg/mL in 150 mM NaCl), incubate for 30 min at room temperature, and rinse and aspirate the Fluorodish 3x with DPBS.
 10. Other excitation, emission, and dichroic filters with comparable properties are possible. For examples, *see (20, 22)*.
 11. Ensure that all solutions, materials, and equipment coming into contact with living cells are sterile.
 12. Ensure that the cells are healthy and actively growing (recommended confluency: 80-90%; this corresponds to $\sim 1.1 \times 10^5$ cells/cm²).
 13. Regularly check on an inverted light microscope if the cells start to detach. Placing the cells at 37°C will facilitate dispersal.
 14. FBS contains trypsin inhibitors and adding a complete growth medium to the cells will immediately inhibit further trypsin activity. Given that over-trypsinization will decrease cell viability, it is recommended to add the growth medium as soon as the cells detach.
 15. Make sure there are no clumps of cells left (this dramatically reduces transfection efficiency).
 16. Storing the cell suspension for more than 15 minutes at room temperature may reduce cell viability and transfection efficiency.

17. The recommended final cell density can vary between different cell lines. For details, consult the Neon Transfection System supplier's website (<https://www.thermofisher.com/be/en/home/life-science/cell-culture/transfection/neon-transfection-system/neon-transfection-system-cell-line-data.html>).
18. The pulse parameters depend on the cell line used. For details, consult the Neon Transfection System supplier's website (<https://www.thermofisher.com/be/en/home/life-science/cell-culture/transfection/neon-transfection-system/neon-transfection-system-cell-line-data.html>).
19. Considering that a strong electrical field induces pore formation, the presence of antibiotics and antimycotics in the post-electroporation culture medium may reduce the viability of freshly transfected cells.
20. Flp-In™ T-REx™ 293 cells need approximately 2 h to attach to the PEI-coated glass bottom of FD35 Fluorodishes. PEI coating promotes firm attachment of HEK-293 cells to the glass bottom of these imaging dishes. Other cell lines may efficiently attach without such coating or require a different attachment time. Therefore, it is strongly recommended to verify cell attachment (e.g., by using an inverted light microscope) before refreshing the medium.
21. As the import kinetics of po-SoNar and po-cpYFP into peroxisomes are rather slow, it takes about 3 days before these proteins display a predominantly peroxisomal staining pattern (**Fig. 2**).
22. The composition of the assay medium depends on the purpose of the study. Measurements can be done in a complete growth medium or in any other buffer solution suitable for live-cell imaging. However, differences in assay medium composition can

- markedly alter cellular metabolism, and hence the NADPH levels and NAD^+/NADH ratios.
23. Cellular metabolism is directly linked to environmental factors such as temperature, pH, and medium composition. In addition, SoNar and iNAP1c are themselves pH-sensitive. As such, it is essential to control these factors as much as possible. For example, most cell culture media contain sodium bicarbonate, which in the presence of 5% CO_2 has a high buffering capacity at pH 7.4. If the measurements are instead made in an assay media without this buffering agent, CO_2 supplementation is not required.
 24. The main advantage of ratiometric instead of absolute intensity measurements is that the outcome is not affected by the expression levels of the sensors.
 25. The signal intensities should be within the linear dynamic range of the detector (extremely weak or saturated images cannot be quantitatively analyzed). The intensities can be optimized by adjusting the exposure times. However, it is essential to respect the F485/F420 nm exposure time ratios for conditions that need to be compared.
 26. Over-illumination can cause oxidative stress and/or photobleach the fluorophore, especially during time-lapse experiments.
 27. To avoid differences caused by difficult to control environmental factors (e.g., different batches of sera), it is important to collect the images of control and test conditions side-by-side.
 28. Fluorescence microscopy images can also be analyzed and/or modified by using other image analysis software such as ImageJ (<http://rsbweb.nih.gov/ij/>).

29. For a statistically relevant analysis, all experiments should be independently repeated at least 3 times. In addition, it is recommended to collect each time at least 10 random images per condition.
30. Given that po-SoNar and po-cpYFP can be partially mislocalized to the cytosol (**Fig. 2**), it is important to accurately delineate ROIs that coincide with peroxisomes.
31. Given that peroxisomes are mobile organelles, it is not uncommon that they shift position in between the first and the second image. One should be vigilant for such events when selecting ROIs.
32. It is recommended to export the values to an Excel or other spreadsheet program.
33. The statistical analysis can be completed with user-preferred software (e.g., Graphpad Prism). Alternatively, a useful and free website for statistical computation is VassarStats (<http://vassarstats.net/>).
34. Based on our (unpublished) observation that the PTS2-containing amino acid sequence interferes with the fluorescence properties of cpYFP, only intra-compartmental comparisons are possible.
35. LbNOX is a water-forming NADH oxidase from *Lactobacillus brevis* that can be used as a genetic tool to manipulate the NAD⁺/NADH ratio in living cells (**29**), including the peroxisomal one (**Fig. 3A**).
36. DHEA is a non-competitive inhibitor of glucose-6-phosphate dehydrogenase, the rate-limiting enzyme in the pentose phosphate pathway, that can be used to lower intracellular NADPH levels (**30**), including the peroxisomal one (**Fig. 3B**).

Acknowledgments

This work has received funding from the European Union's Horizon 2020 Research and Innovation Programme under the Marie Skłodowska-Curie grant agreement No 812968, the KU Leuven (C14/18/088), and the Research Foundation – Flanders (G091819N). CL was supported by the Research Foundation – Flanders (1213620N), MH was supported by the Egyptian Government Scholarship Program, and HL was a recipient of a doctoral fellowship from the China Scholarship Council (201906790005).

References

1. Nakamura M, Bhatnagar A, Sadoshima J (2012) Overview of pyridine nucleotides. *Circ Res* 111:604-610. doi: 10.1161/CIRCRESAHA.111.247924
2. Xiao W, Wang RS, Handy DE, Loscalzo J (2018) NAD(H) and NADP(H) redox couples and cellular energy metabolism. *Antioxid Redox Signal* 28:251-272. doi: 10.1089/ars.2017.7216
3. Yang Y, Sauve AA (2016) NAD⁺ metabolism: bioenergetics, signaling and manipulation for therapy. *Biochim Biophys Acta* 1864:1787-1800. doi: 10.1016/j.bbapap.2016.06.014
4. Xie N, Zhang L, Gao W, Huang C, Huber PE, Zhou X, Li C, Shen G, Zou B (2020) NAD⁺ metabolism: pathophysiologic mechanisms and therapeutic potential. *Signal Transduct Target Ther* 5:227. doi: 10.1038/s41392-020-00311-7
5. Covarrubias AJ, Perrone R, Grozio A, Verdin E (2021) NAD⁺ metabolism and its roles in cellular processes during ageing. *Nat Rev Mol Cell Biol* 22:119-141. doi: 10.1038/s41580-020-00313-x

6. Bradshaw PC (2019) Cytoplasmic and mitochondrial NADPH-coupled redox systems in the regulation of aging. *Nutrients* 11:504. doi: 10.3390/nu11030504
7. Rather GM, Pramono AA, Szekely Z, Bertino JR, Tedeschi PM (2021) In cancer, all roads lead to NADPH. *Pharmacol Ther* 226:107864. doi: 10.1016/j.pharmthera.2021.107864
8. Kupfer D, Munsell T (1968) A colorimetric method for the quantitative determination of reduced pyridine nucleotides (NADPH and NADH). *Anal Biochem* 25:10-6. doi: 10.1016/0003-2697(68)90075-4
9. Chamchoy K, Pakotiprapha D, Pumirat P, Leartsakulpanich U, Boonyuen U (2019) Application of WST-8 based colorimetric NAD(P)H detection for quantitative dehydrogenase assays. *BMC Biochem* 20:4. doi: 10.1186/s12858-019-0108-1
10. Xie W, Xu A, Yeung ES (2009) Determination of NAD⁺ and NADH in a single cell under hydrogen peroxide stress by capillary electrophoresis. *Anal Chem* 81:1280-1284. doi: 10.1021/ac802249m
11. Pálfi M, Halász AS, Tábi T, Magyar K, Szöke E (2004) Application of the measurement of oxidized pyridine dinucleotides with high-performance liquid chromatography-fluorescence detection to assay the uncoupled oxidation of NADPH by neuronal nitric oxide synthase. *Anal Biochem* 326:69-77. doi: 10.1016/j.ab.2003.11.010
12. Caruso R, Campolo J, Dellanoce C, Mariele R, Parodi O, Accinni R (2004) Critical study of preanalytical and analytical phases of adenine and pyridine nucleotide assay in human whole blood. *Anal Biochem* 330:43-51. doi: 10.1016/j.ab.2004.03.063

13. Yoshino J, Imai S (2013) Accurate measurement of nicotinamide adenine dinucleotide (NAD⁺) with high-performance liquid chromatography. *Methods Mol Biol* 1077:203-215. doi: 10.1007/978-1-62703-637-5_14
14. Shabalin K, Nerinovski K, Yakimov A, Kulikova V, Svetlova M, Solovjeva L, Khodorkovskiy M, Gambaryan S, Cunningham R, Migaud ME, Ziegler M, Nikiforov A (2018) NAD metabolome analysis in human cells using ¹H NMR spectroscopy. *Int J Mol Sci* 19:3906. doi: 10.3390/ijms19123906
15. Lu W, Wang L, Chen L, Hui S, Rabinowitz JD (2018) Extraction and quantitation of nicotinamide adenine dinucleotide redox cofactors. *Antioxid Redox Signal* 28:167-179. doi: 10.1089/ars.2017.7014
16. Petucci C, Culver JA, Kapoor N, Sessions EH, Divlianska D, Gardell SJ (2019) Measurement of pyridine nucleotides in biological samples using LC-MS/MS. *Methods Mol Biol* 1996:61-73. doi: 10.1007/978-1-4939-9488-5_7
17. Braidy N, Villalva MD, Grant R (2021) NADomics: Measuring NAD⁺ and related metabolites using liquid chromatography mass spectrometry. *Life (Basel)* 11:512. doi: 10.3390/life11060512
18. Chorny S, IJlst L, van Roermund CWT, Wanders RJA, Waterham HR (2021) Peroxisomal metabolite and cofactor transport in humans. *Front Cell Dev Biol* 8:613892. doi: 10.3389/fcell.2020.613892
19. Zhao Y, Zhang Z, Zou Y, Yang Y (2018) Visualization of nicotine adenine dinucleotide redox homeostasis with genetically encoded fluorescent sensors. *Antioxid Redox Signal* 28:213-229. doi: 10.1089/ars.2017.7226

20. Zhao Y, Hu Q, Cheng F, Su N, Wang A, Zou Y, Hu H, Chen X, Zhou HM, Huang X, Yang K, Zhu Q, Wang X, Yi J, Zhu L, Qian X, Chen L, Tang Y, Loscalzo J, Yang Y (2015) SoNar, a highly responsive NAD⁺/NADH sensor, allows high-throughput metabolic screening of anti-tumor agents. *Cell Metab* 21:777-789. doi: 10.1016/j.cmet.2015.04.009
21. Zhao Y, Wang A, Zou Y, Su N, Loscalzo J, Yang Y (2016) In vivo monitoring of cellular energy metabolism using SoNar, a highly responsive sensor for NAD⁺/NADH redox state. *Nat Protoc* 11:1345-1359. doi: 10.1038/nprot.2016.074
22. Tao R, Zhao Y, Chu H, Wang A, Zhu J, Chen X, Zou Y, Shi M, Liu R, Su N, Du J, Zhou HM, Zhu L, Qian X, Liu H, Loscalzo J, Yang Y (2017) Genetically encoded fluorescent sensors reveal dynamic regulation of NADPH metabolism. *Nat Methods* 14:720-728. doi: 10.1038/nmeth.4306
23. Schwarzländer M, Wagner S, Ermakova YG, et al (2014) The 'mitoflash' probe cpYFP does not respond to superoxide. *Nature* 514:E12-E14. doi: 10.1038/nature13858
24. Fransen M (2014) HaloTag as a tool to investigate peroxisome dynamics in cultured mammalian cells. *Methods Mol Biol* 1174:157-170. doi: 10.1007/978-1-4939-0944-5_10
25. Lismont C, Walton PA, Fransen M (2017) Quantitative monitoring of subcellular redox dynamics in living mammalian cells using roGFP2-based probes. *Methods Mol Biol* 1595:151-164. doi: 10.1007/978-1-4939-6937-1_14
26. Lennicke C, Cochemé HM (2021) Redox metabolism: ROS as specific molecular regulators of cell signaling and function. *Mol Cell* 81:3691-3707. doi: 10.1016/j.molcel.2021.08.018
27. Brees C, Fransen M (2014) A cost-effective approach to microporate mammalian cells with the Neon Transfection System. *Anal Biochem* 466:49-50. doi: 10.1016/j.ab.2014.08.017

28. Nordgren M, Wang B, Apanasets O, Brees C, Veldhoven PP, Franssen M (2012) Potential limitations in the use of KillerRed for fluorescence microscopy. *J Microsc* 245:229-235. doi: 10.1111/j.1365-2818.2011.03564.x
29. Titov DV, Cracan V, Goodman RP, Peng J, Grabarek Z, Mootha VK (2016) Complementation of mitochondrial electron transport chain by manipulation of the NAD⁺/NADH ratio. *Science* 352:231-235. doi: 10.1126/science.aad4017
30. Gordon G, Mackow MC, Levy HR (1995) On the mechanism of interaction of steroids with human glucose 6-phosphate dehydrogenase. *Arch Biochem Biophys* 318:25-29. doi: 10.1006/abbi.1995.1199

Figure Captions

Fig. 1 Diagram showing the principle of SoNar- and iNAP1-based sensors. F420, fluorescence intensity at 420 nm excitation; F485, fluorescence intensity at 485 nm excitation.

Fig. 2 Subcellular localization of po-SoNar, po-cpYFP, po-iNAP1, and po-iNAPc. Flp-InTM T-RExTM 293 cells were transfected with a plasmid encoding po-mCherry, a fluorescent peroxisomal marker protein, and (A) po-SoNar, (B) po-cpYFP, (C) po-iNAP1, or (D) po-iNAPc. The cells were cultured in regular MEM α medium for three days and then imaged by epifluorescence microscopy. Representative images are shown. The boxed areas in the upper panels are enlarged in the lower panels. Scale bar, 10 μ m.

Fig. 3 Functional validation of po-SoNar and po-iNAP1. Flp-In T-REx 293 cells were transfected with a plasmid encoding (A) po-SoNar or po-cpYFP, in combination (+) or not (-) with a plasmid coding for LbNOX, a *Lactobacillus brevis* NADH oxidase, or (B) po-iNAP1 or po-iNAPc. The cells were cultured in regular MEM α medium for 3 days. Next, (i) the F485/F420 response ratios of the sensors were measured, (ii) the cells expressing po-iNAP1 or po-iNAPc were incubated for 30 minutes in regular medium supplemented with 200 μ M dehydroepiandrosterone (DHEA), an inhibitor of the pentose phosphate pathway, and (iii) the F485/F420 response ratios of po-iNAP1 and po-iNAPc were measured again. The pH-corrected values for po-SoNar and po-iNAP1 in the treatment (+) groups were plotted as fold change compared to the average value of the corresponding control (-) groups. The bottom and top of each box represent the 25th and 75th percentile values, respectively; the horizontal line inside each box represents the median; and the horizontal lines below and above each box denote the minimum and the maximum, respectively. The data were derived from 30 individual images from 3 independent experiments, each comprising 10 fields of view. Differences in response ratios between the treatment (+) and

corresponding control (-) conditions were statistically compared using the Mann-Whitney test (****, $p < 0.0001$). (A) Expression of LbNOX increases the peroxisomal free NAD^+/NADH ratios. (B) DHEA-mediated inhibition of the pentose phosphate pathway decreases the peroxisomal NADHP levels.

Table 1 Filter cubes to image cells expressing SoNar, cpYFP, iNAP1 or iNAPc

Sensor	Parameter	Filter cube(s)
SoNar	NAD ⁺	F485
	NADH	F420
cpYFP	pH fluctuations	F420 & F485
iNAP1	NADPH	F420
	NADPH-free	F485
iNAPc	pH fluctuations	F420 & F485

Fig. 1

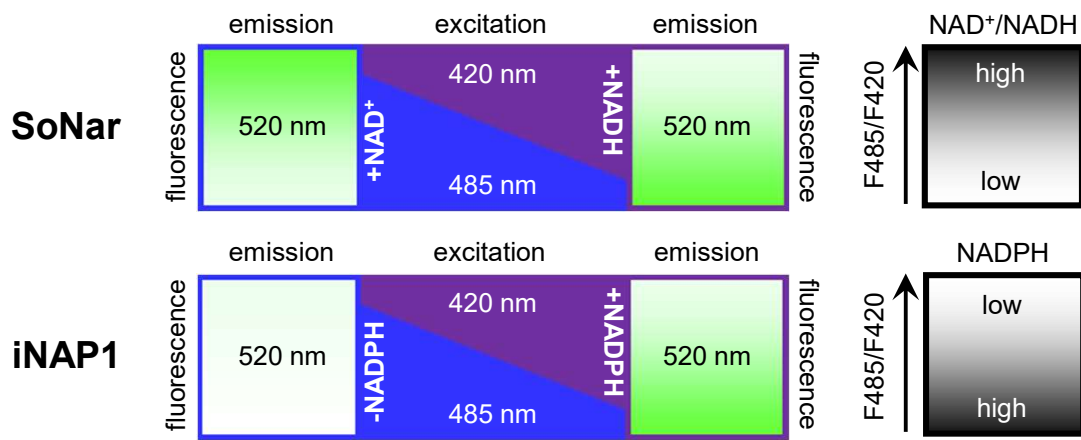


Fig. 2

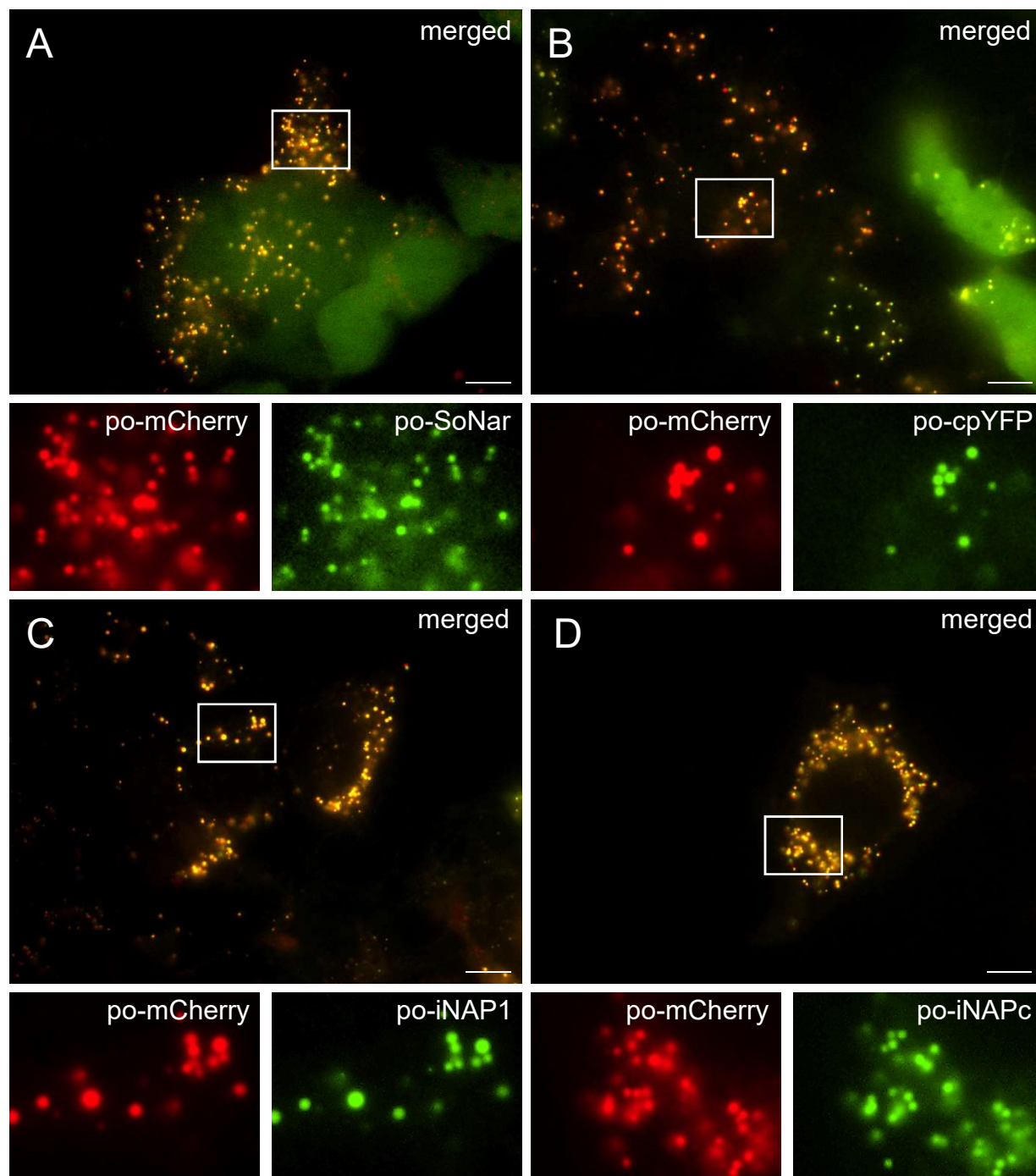


Fig. 3

